Clays and Clay Minerals, Vol. 47, No. 3, 329–337, 1999.

DISTINGUISHING BETWEEN SURFACE AND BULK DEHYDRATION-DEHYDROXYLATION REACTIONS IN SYNTHETIC GOETHITES BY HIGH-RESOLUTION THERMOGRAVIMETRIC ANALYSIS

ROBERT G. FORD† AND PAUL M. BERTSCH

Advanced Analytical Center for Environmental Science, Savannah River Ecology Laboratory, University of Georgia, P.O. Drawer E, Aiken, South Carolina 29802, USA

Abstract—Synthetic goethites studied by high-resolution thermogravimetry (HRTGA) show variability in surface characteristics and structural stability as a function of aging conditions. Goethites were synthesized at either pH 6 or 11, at temperatures of 40 or 70°C, and in the presence or absence of sorbed Mn or Pb. Data from HRTGA analysis revealed at least four distinct weight-loss events near goethite dehydroxylation that relate to 1) three events involving the evolution of water associated with surface Fe-O functional groups and 2) bulk dehydroxylation of goethite during transformation to hematite. The relative mass of evolved surface and bulk structural water was related to the predominant particle morphology as determined by transmission electron microscopy (TEM). Differentiation of surface and bulk decomposition reactions allowed the identification of bulk structural dehydroxylation. Goethite crystallinity, estimated by the bulk dehydroxylation temperature, appeared to depend on the kinetics of crystallization. This trend was most evident for systems aged at pH 11 and 40°C. Greater concentrations of coprecipitated Mn or Pb dramatically improved goethite crystallinity as indicated by higher dehydroxylation temperatures and smaller widths of the (110) Bragg reflection. Comparison of bulk dehydroxylation temperatures for these samples to other preparations suggests that structural defects predominated over the effects of particle size and Mn/Pb substitution in determining goethite thermal stability. A conceptual model is proposed to account for the disparate dehydroxylation profiles displayed by goethites of varying crystallinity.

Key Words—Crystallinity, Dehydroxylation, Goethite, Thermogravimetry, Nonstoichiometric Water, TEM, XRD.

INTRODUCTION

Studies with synthetic goethite are commonly used to develop models for the surface chemistry of soil goethites. The morphology and structure of synthetic and soil goethites can vary widely (Schwertmann and Taylor, 1989; Schwertmann, 1990). Variability in particle morphology is due to the preferential development of different crystallographic planes during growth (Domingo *et al.*, 1994). This results in particle surfaces populated by Fe-O functional groups with different degrees of coordination to the bulk structure and, therefore, variable surface reactivity (Parfitt *et al.*, 1975; Rochester and Topham, 1978). Hiemstra *et al.* (1989) proposed that changes in the population of reactive sites at the goethite surface influence the sorption of ionic species. For example, Colombo *et al.* (1994) found that phosphate adsorption onto hematite, a structurally related iron oxide, is influenced by the predominant particle morphology. In addition, molecular statics calculations of goethite surface structures predicted the presence of several (oxo)hydroxo functional groups with varying degrees of reactivity (Rustad *et al.*, 1996).

The atomic structure of synthetic goethites may deviate from that of the ideal structure, α-FeOOH. Possible deviations for pure goethites include excess structural OH and Fe cation deficiencies (Wolska and Schwertmann, 1993). In addition, structural defects such as stacking faults or intergrowths were also identified (Schwertmann, 1984a; Mann *et al.*, 1985; Cornell and Giovanoli, 1986). These defect structures reduce the overall stability of the mineral and may be nucleation sites for dissolution or sorption reactions (Maurice *et al.*, 1995). Several studies showed that goethites with a high population of structural defects are more susceptible to acid attack during dissolution (Cornell *et al.*, 1974; Schwertmann, 1984a). In addition, slowly reversible metal sorption to synthetic goethite was attributed to slow diffusion of metals from micropores (Bruemmer *et al.*, 1988). This internal microporous network is likely formed by the propagation of structural defects during crystal growth (Cornell and Giovanoli, 1986).

Numerous studies characterized the variable morphologies and crystallinity imparted to synthetic goethites as a function of the conditions controlling transformation from ferrihydrite (Cornell and Giovanoli, 1985; Schwertmann *et al.*, 1985; Schulze and Schwertmann, 1987). The term crystallinity may embody several crystallite characteristics such as particle size and

† Current Address: University of Delaware, Department of Plant and Soil Sciences, Newark, Delaware 19717, USA.

Copyright © 1999, The Clay Minerals Society

https://doi.org/10.1346/CCMN.1999.0470309 Published online by Cambridge University Press

structural perfection; however, herein we define crystallinity as the presence of structural defects affecting the thermal stability of crystallites. For goethite, it was generally shown that crystals with fewer defects are the result of either slow crystal growth at low temperature or by hydrothermal aging (Schulze, 1984; Schwertmann, 1984a). Higher aging temperatures purportedly improve crystallinity by providing the energy necessary to heal structural imperfections (Schulze and Schwertmann, 1987). Slow crystal growth apparently leads to crystallites with fewer defects by reducing the likelihood of misorientation during the addition of growth units (Mann *et al.*, 1985).

The kinetics of the transformation of ferrihydrite to goethite is influenced by several variables including pH, temperature, and the presence of foreign ions (Cornell *et al.*, 1989). Schwertmann and Murad (1983) and Schwertmann *et al.* (1985) showed that transformation rates are slowed with decreasing pH and temperature. Transformation to goethite is also retarded by metal sorption to ferrihydite (Cornell *et al.*, 1989; Giovanoli and Cornell, 1992). For example, studies showed improved goethite crystallinity with increasing levels of Al sorption during crystal growth (Schulze and Schwertmann, 1984; Schwertmann, 1984a).

The crystallinity of soil and synthetic goethites was commonly characterized by X-ray diffraction (XRD) or infrared (IR) spectroscopy (Kuhnel *et al.*, 1975; Schulze and Schwertmann, 1984; Schwertmann *et al.*, 1985). XRD measures the degree of long-range order within crystal structures, thus defects are indicated by a decrease in the size of coherently diffracting domains (Reynolds, 1989). Domain sizes are determined based on the width of Bragg reflections, broader peaks being indicative of poorer crystallinity. However, peak broadening may also be influenced by particle size, and it may be difficult to separate the influence of the two characteristics (Schwertmann *et al.*, 1985; Cambier, 1986a). IR spectroscopy measures the short-range structural order in goethite by probing hydroxyl and lattice vibrational modes (Cambier, 1986b). This provides a more direct determination of the local structure leading to poor crystallinity, but results may also be influenced by particle morphology (Cambier, 1986a).

Both techniques provide information on how defects occur within the crystal, but they do not directly measure instability imparted by these defects. The thermal stability of goethites with varying crystallinity is best measured via thermoanalytical techniques. Specifically, the temperature where bulk structural dehydroxylation occurs, i.e. goethite transforms to hematite, is a measure of the stability of the structure as a whole (Goss, 1987). In addition, characteristics of the goethite surface and the bulk structure may be probed under favorable experimental conditions (Mackenzie *et al.*, 1981). The recent availability of high-resolution thermogravimetric analyzers has expanded the capabilities of thermal analysis for the characterization of mineral surfaces.

The objective of this research is to examine the influence of crystallization conditions on the surface properties and thermal stability of synthetic goethites formed by transformation of ferrihydrite. It is presumed that the rate of transformation has a profound influence on the surface and bulk properties of goethite crystallites. To test this hypothesis, we systematically varied the transformation rate through adjustment of pH and temperature of aging and by introducing Mn or Pb at various concentrations as a contaminant within the initial ferrihydrite coprecipitate. Bulk and surface properties of the goethites produced during aging was characterized by high-resolution thermogravimetric analysis (HRGTA). Transmission electron microscopy (TEM) was employed to assess differences in crystallite morphology on observed surface characteristics. Differences in the thermal stability or crystallinity of goethite was compared to XRD results. The specific goal of this research is to show that HRTGA can differentiate surface and bulk structural characteristics of synthetic goethites.

MATERIALS AND METHODS

Precipitation and aging

Precipitates of Fe^{3+} in the presence or absence of coprecipitated Mn^{2+} or Pb^{2+} were generated by the addition of 1 M low-CO_2 NaOH with a Radiometer automatic titration system to acidified solutions of the metal salt (TTT 80 titrator unit, ABU 80 autoburette with 10 ml burette) at room temperature in a Teflon container. In all cases, starting solutions consisted of 20 ml of 0.1 M $Fe(NO_3)_3$, 140 ml of 0.1 M $NaNO_3$, and 20 ml of either a $MnCl_2$ or $Pb(NO_3)_2$ solution to give a final metal concentration between 0.05–1.0 mM relative to Fe which was set at 10 mM. All stock metal solutions were made up in 0.1 M HNO_3 and 0.1 M $NaNO_3$. Base was then added to these starting solutions (starting pH = 1.6–1.7) over 1 h to an end-point of either pH 6 or 7, and the resultant precipitate slurries were held at this pH for an additional 2 h to insure near-equilibrium adsorption of coprecipitated metals and complete hydrolysis of solution Fe. After this period, pH 6 systems were placed in a water bath at 40 or 70°C for aging, and pH 7 systems were titrated to and held at pH 11 for 1.5 h prior to aging under the same conditions (200 ml final volume in each case). Prior to aging at 40 or 70°C, the precipitates were primarily composed of ferrihydrite. Thus, during the aging period two processes might occur: 1) transformation of ferrihydrite to goethite and hematite and 2) crystal healing of the transformed phases by hydrothermal treatment.

At pH 11, the hydroxyl ion was present at a sufficient concentration to buffer the system during aging,

https://doi.org/10.1346/CCMN.1999.0470309 Published online by Cambridge University Press

Table 1. Aging parameters, extractable Fe fractions ($[Fe]_o/[Fe]_t$), and temperatures of goethite dehydration-dehydroxylation events for Fe oxide precipitates. Temperatures for dehydration-dehydroxylation events were determined using peak-fitting method described in the text.

Sample ID	$[Me^{2+}]$ mM	Aging T (°C)	Aging pH	Aging time (h)	$[Fe]_o/[Fe]_t$	$\equiv S_1OH$ (°C)	$\equiv S_2OH$ (°C)	$\equiv S_3OH$ (°C)	$T_{OH,b}$ (°C)
FeB76	0	70	6	380	0.26	215	240	259.6	275.4
FePb1B76	0.05	70	6	380	0.07	204.6	229.4	253	279.3
FePb1A76	0.5	70	6	379	0.28	206.7	230.7	256.9	273.7
FePb1C76	0.5	70	6	382	0.25	214.2	235.7	259.9	276.5
FePb1D76	0.5	70	6	380	0.23	212.3	236.8	258.2	272.3
FeMn1A76	0.5	70	6	378	0.2	201.7	224.8	249.5	273
FeB71	0	70	11	25	0.07	213.9	225	242.6	269.7
FeC71	0	70	11	24.3	0.01	209.4	230	251.9	268
FeD71	0	70	11	25.8	0.01	205.8	228.7	254.8	269
FePb1B71	0.5	70	11	26.5	0.1	204	226.2	239.9	265.8
FePb2A71	0.75	70	11	26.5	0.14	214.9	236.4	254.8	270
FePb2B71	0.75	70	11	27	0.17	216.7	233.3	255.4	270.8
FePb3A71	1	70	11	27.7	—	212.2	229.9	252.9	270.6
FeA41	0	40	11	379	—	203.1	224.3	241.4	248.2
FePb1A41	0.5	40	11	481	0.06	216.9	230.6	246.2	260.1
FePb2A41	0.75	40	11	481	0.08	213.3	227.5	248.7	267
FePb3A41	1	40	11	475	0.12	204.5	220.2	246.7	270.2
FeMn1A41	0.5	40	11	476	0.03	219.4	231.9	243.2	259.8
FeMn2A41	0.75	40	11	483	0.08	200	220.2	244.3	266.7
FeMn3A41	1	40	11	481	0.15	203.6	223.1	247.6	272.1
FeB46	0	40	6	1437	0.63	206	228.5	248.1	268.4
FeMn1B46	0.05	40	6	1053	0.85	203.2	220	240.4	276.4
FeMn1A46	0.5	40	6	1008	0.88	201.1	225.2	255.4	273.5

and deviations were $<\pm 0.5$ pH units. For the pH 6 systems, changes in pH were mitigated either by daily manual adjustments with 0.1 M NaOH or the addition of 2-(4-morpholino)-ethane sulfonic acid (MES) or piperazine-N,N′-bis[2-ethanesulfonic acid] (PIPES) as buffers (5 mM). Comparison of aging in the presence or absence of MES or PIPES showed minor influence of the buffer on metal partitioning and rate of crystallization. However, the presence of MES increased the relative fraction of hematite in the systems free of Mn or Pb.

Solid phase characterization

Table 1 summarizes the aging conditions and time, the ammonium oxalate extractable fraction (Schwertmann and Cornell, 1991), and data from thermogravimetric analysis. Note that the fraction of ferrihydrite remaining in the solids varied for systems aged at different pH and temperature. All samples were characterized by the methods given below prior to extraction of ferrihydrite.

Bulk mineralogy was characterized by HRTGA, powder XRD, and for select samples by TEM. HRTGA involved an atmosphere of He on freeze-dried powder samples (~5 mg) using a TA Instruments Hi-Res TGA 2950 over a temperature range of 40 to 700°C. High resolution is achieved by continuous monitoring of weight-loss via computer control and automatic reduction of the heating rate upon weight-loss detection, thus allowing optimized resolution of multiple closely-spaced decomposition reactions. The resolution of weight-loss events is optimized by adjusting resolution and sensitivity settings to achieve near-isothermal conditions at each weight-loss event (Anonymous, 1997). Instrumental parameters were: (1) maximum heating rate = 20°C min^{-1}, (2) resolution = 5.0, and (3) sensitivity = 1.0. Heating rate was automatically reduced to values <1°C min^{-1} for large weight-loss events such as the goethite bulk dehydroxylation. In some cases, samples were extracted with 0.4 M HCl for 30 min to remove ferrihydrite (Cornell and Schneider, 1989), then washed with milli-Q H_2O and dried prior to analysis by HRTGA.

XRD analyses used oriented clay mineral aggregates and a Scintag XDS 2000 diffractometer employing CuKα radiation and an intrinsic germanium detector. Samples were scanned over 2θ = 10–70° with a 0.3 °2θ step size (3.6 sec/step). TEM analysis was performed with a JEOL 2010 transmission electron microscope at an accelerating voltage of 200 keV. Samples were prepared by drying a drop of dilute suspension on a holey carbon film supported by a copper grid.

RESULTS AND DISCUSSION

Morphology and surface dehydration-dehydroxylation

A complex series of weight-loss events prior to bulk dehydroxylation was observed during characterization of goethite by HRTGA (Figure 1). These features are more easily visualized by the derivative of the weight-

https://doi.org/10.1346/CCMN.1999.0470309 Published online by Cambridge University Press

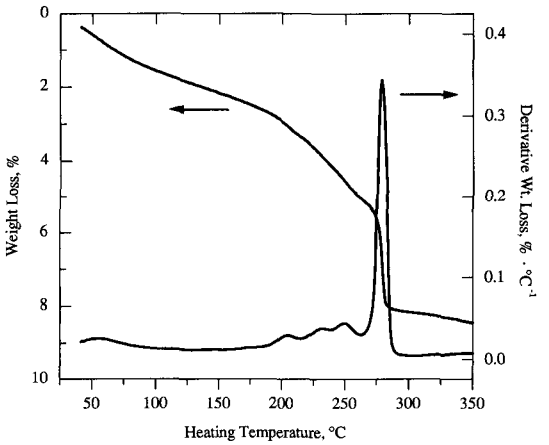

Figure 1. Thermogravimetric analysis of goethite synthesized from a Pb-ferrihydrite coprecipitate. The left-hand scale indicates the mass loss (wt. %) during heating, and the right-hand scale is the derivative of the weight-loss curve. Aging conditions: pH 6, 70°C, 0.05 mM Pb, 10 mM Fe, 0.14 M $NaNO_3$, 5 mM MES, 380 h.

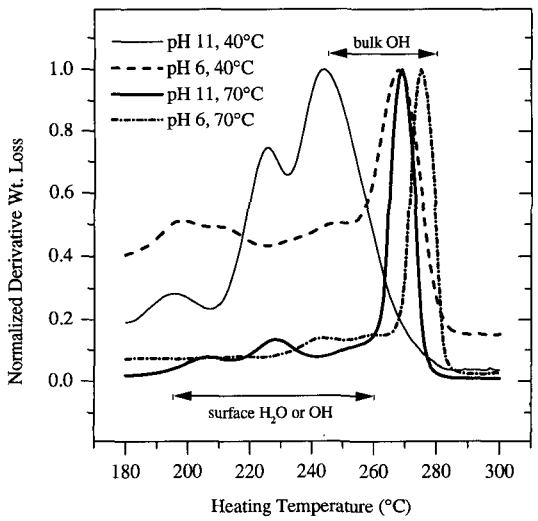

Figure 2. HRTGA thermograms showing goethite decomposition reactions for samples aged in the absence of Mn or Pb under different pH and temperature. Temperature ranges for surface and bulk dehydration-dehydroxylation events are indicated.

loss curve, or thermogram; see the scale to the right in Figure 1. Peak maxima coincide with a maximum rate of weight-loss, whereas the minima between peaks occur during the transition between weight-loss events. Multiple weight-loss events immediately preceding bulk dehydroxylation are attributed to dehydration or dehydroxylation of surface Fe (oxo)hydroxo functional groups and similar events were observed in several investigations with goethites of varying crystallinity (Paterson and Swaffield, 1980; Fey and Dixon, 1981; Mackenzie *et al.*, 1981; Schulze and Schwertmann, 1984; Schwertmann, 1984b; Schulze and Schwertmann, 1987; Gasser *et al.*, 1996). In this study, all goethites showed this complex weight-loss pattern to varying degrees as illustrated by thermograms for samples prepared in the absence of Mn or Pb and aged at different pH and temperature (Figure 2). For comparison between samples, we modeled the goethite thermogram within the temperature range of 180–300°C as the evolution of water from three distinct surface structural groups followed by bulk dehydroxylation.

The conceptual model of Paterson and Swaffield (1980) based on the identification of surface hydroxyls coordinated to one, two, or three Fe atoms within the bulk structure (Russell *et al.*, 1974; Sposito, 1984) was adopted. Hereafter, we label these hydroxyls as $=S_1OH$, $=S_2OH$, and $=S_3OH$. Based on our study, we cannot determine if the evolved water is true dehydroxylation or from evolution of hydrogen-bonded H_2O molecules. However, Paterson and Swaffield (1980) showed that these decomposition reactions are partially reversible, suggesting specifically coordinated water molecules consistent with the ferrihydrite surface structural model proposed by Manceau and Gates (1997). Regardless of the exact surface structure, analysis of the goethites from this study clearly indicates that these weight-loss events are distinct from dehydroxylation of the bulk structure.

Each thermogram was decomposed using Gaussian peaks superimposed over a linear baseline to derive information on the temperature and weight loss of each event. The non-linear curve fitting routine of the GRAMS/386 software package (Galactic Industries Corporation) was used to model the thermogram. For example, decomposition of the thermogram in Figure 1 at 180–300°C is displayed in Figure 3. As shown below, the goethites synthesized at pH 6 and 70°C were well-crystallized single crystals and the resolution of weight-loss events was optimal. Analysis of these thermograms (six total) constrained the location and peak width for weight-loss events in poorly-resolved thermograms for goethites of more variable morphology synthesized at other pH and temperatures. Specifically, the widths at half-height for 'peaks' attributable to surface events were constrained to be ≤25°C, and their maxima were constrained to fall within the following temperature regions: $=S_1OH$, 195–215°C; $=S_2OH$, 220–240°C; and $=S_3OH$, 240–260°C. No constraints were placed on the width or location of the weight-loss event attributed to bulk dehydroxylation. This analysis approach assumes that surface decomposition reactions were relatively invariant regardless of differences in bulk crystallinity for all goethites. As shown below, this assumption was crucial for peak fitting for samples where there is significant overlap between decomposition of the $=S_3OH$ surface group and bulk dehydroxylation.

https://doi.org/10.1346/CCMN.1999.0470309 Published online by Cambridge University Press

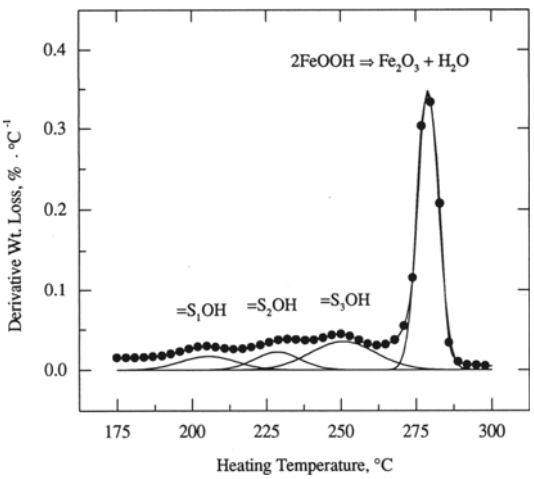

Figure 3. Decomposition of the HRTGA thermogram showing dehydration or dehydroxylation of three surface waters preceding bulk dehydroxylation of goethite. Aging conditions: pH 6, 70°C, 0.05 mM Pb, 10 mM Fe, 0.14 M $NaNO_3$, 5 mM MES, 380 h.

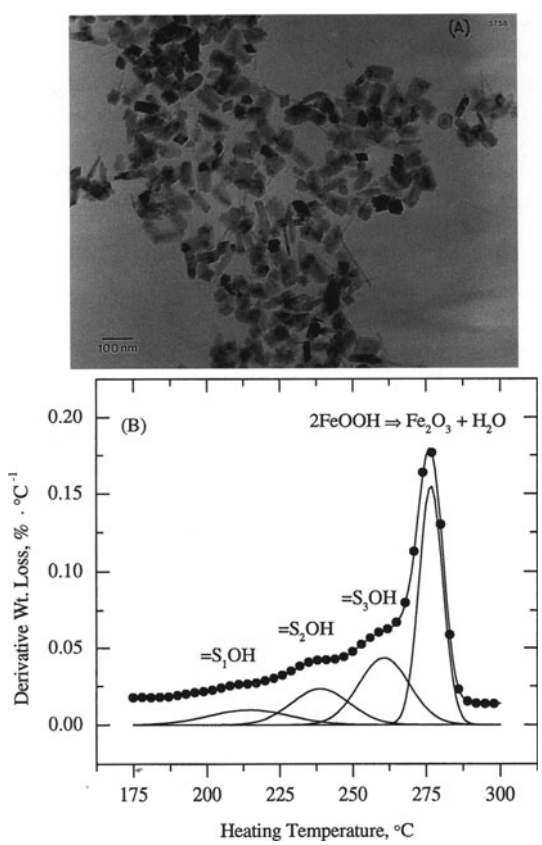

Figure 4. Characterization by (A) TEM and (B) HRTGA of goethite produced by aging a Pb-ferrihydrite coprecipitate (0.5 mM Pb) at pH 6 and 70°C for 380 h. The best-fit peaks for dehydration-dehydroxylation of $=S_1OH$, $=S_2OH$, and $=S_3OH$ and $T_{OH,b}$ are shown below the thermogram.

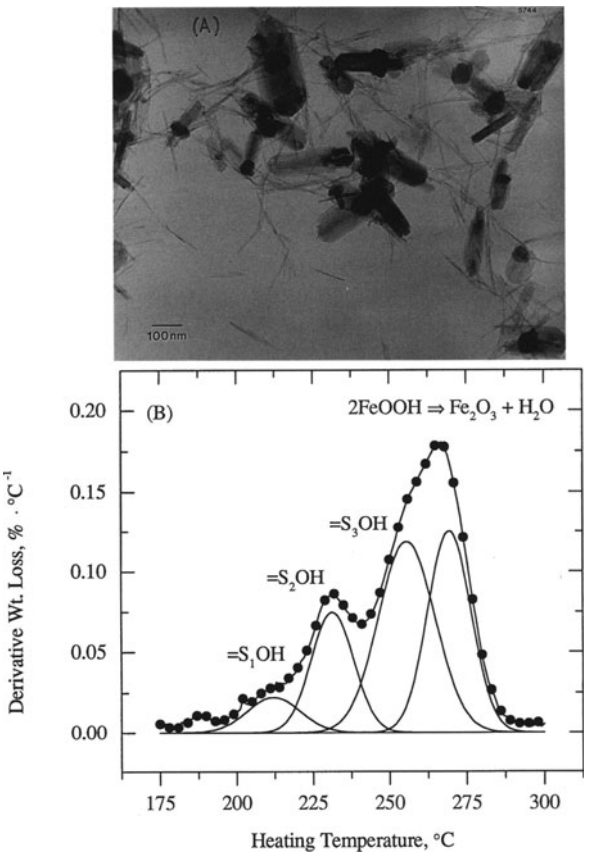

Figure 5. Results of (A) TEM and (B) HRTGA analysis of goethite produced by aging a Pb-ferrihydrite coprecipitate (0.5 mM Pb) at pH 11 and 70°C for 26.5 h. The decomposition of weight-loss events due to surface and bulk dehydration-dehydroxylation is shown below the thermogram.

The morphology and crystallinity of the goethites are related to the aging pH. TEM inspection showed that goethite formed at pH 6 and 70°C appeared highly crystalline (Figure 4A). The mineralogy of this material consists of ~25% ferrihydrite, minor amounts of hematite and a predominance of short lath-like goethite crystals with particle dimensions of 20 × 100 nm. High-resolution TEM analysis of goethite crystallites showed no defects (data not shown). The thermogram for this sample showed clearly resolved surface and bulk structural dehydration-dehydroxylation events (Figure 4B). The thermograms presented in Figures 3 and 4B are representative of the thermal behavior of all samples aged at pH 6. Regardless of the temperature of aging, the bulk dehydroxylation event was easily discerned from surface dehydration-dehydroxylation events during data analysis.

In contrast, the morphology of goethites formed at pH 11 was more variable. For example, Figure 5 shows goethite formed at pH 11 and 70°C in the presence of 0.5 mM Pb. This sample contained ~10% ferrihydrite, goethite, and minor amounts of hematite.

https://doi.org/10.1346/CCMN.1999.0470309 Published online by Cambridge University Press

However, there appears to be two predominant goethite morphologies: (1) acicular crystals with widths of ~5 nm and lengths varying from 40 to 150 nm (*c* axis), and (2) multi-domainic lath-like crystals ~30–160 nm wide and 100–300 nm long. TEM showed that the larger crystals possessed multiple domains parallel to the *c* axis with particle dimensions similar to the individual acicular crystals (data not shown). The thermogram for this sample contrasted with the goethite sample aged at pH 6 in that surface dehydration-dehydroxylation contributed more to the overall weight loss (Figure 5B). This thermogram is representative of the other samples aged at pH 11. Surface dehydration-dehydroxylation events were not always clearly resolved from bulk dehydroxylation, thus requiring a constraint of temperature of surface-decomposition weight loss during peak fitting.

Systematic differences in the surface-weight losses *vs.* bulk dehydroxylation for goethites formed at pH 6 and 11 appear related to the predominant particle morphology developed during aging. Examination of particle development at pH 6 (Figure 4A), suggested that the bulk structure has a greater contribution to the overall hydroxyl population. A simple calculation, assuming an average parallelepiped particle geometry with dimensions 30 × 30 × 100 nm, provides an estimate that ~5% of the unit cells (a = 0.4602 nm, b = 0.9952 nm, c = 0.3021 nm; Sampson, 1969) is located at the particle surface. In contrast, samples synthesized at pH 11 contained a larger proportion of surface (oxo)hydroxo functional groups, consistent with the predominance of acicular crystals or of domains of similar size in larger particles (Figure 5A). Assuming parallelepipeds with average dimensions of 5 × 5 × 100 nm, ~27% of the unit cells are located at the particle surface. These trends were observed also for goethites synthesized at 40°C, where HRTGA showed a greater contribution of surface hydroxyls to the overall dehydration-dehydroxylation for samples aged at pH 11 (*e.g.*, see Figure 2). These findings are consistent with Forsyth *et al.* (1968) and Goss (1987) where water in excess of stoichiometric predictions was measured for goethite dehydroxylation.

Bulk dehydroxylation and goethite crystallinity

The temperature of bulk dehydroxylation was previously used as a measure of goethite crystallinity (*e.g.*, Schulze and Schwertmann, 1984; Schwertmann *et al.*, 1985). However, the determination of this parameter may be complicated for samples displaying multiple weight-loss events over a narrow temperature region. Previous researchers generally employed the temperature of the last decomposition peak or an average temperature for all decomposition events as the true dehydroxylation temperature (Schulze and Schwertmann, 1984; Schulze and Schwertmann, 1987). Schwertmann (1984b) argued that multiple transitions observed during thermal analysis of synthetic goethites by differential thermal analysis (DTA) are characteristic of discrete *bulk* dehydroxylation events. This interpretation is not supported by Paterson and Swaffield (1980) who showed that weight-loss events immediately preceding bulk dehydroxylation are reversible following temperature reduction and re-equilibration within the furnace. True bulk dehydroxylation reversibility was not demonstrated for goethite. There is no obvious mechanism to explain solid-state conversion of hematite to the original goethite by cooling. Thus, the multiple dehydroxylation processes previously observed for goethite can be attributed to a combination of surface and bulk decomposition reactions.

Using the analysis approach outlined above to determine a bulk dehydroxylation event, it is shown that various aging conditions significantly influenced goethite thermal stability and particle morphology. The variability in the temperature of bulk dehydroxylation ($T_{OH,b}$) appears to be partially dependent on the pH and temperature of aging. Values determined for $T_{OH,b}$ and temperatures for surface dehydration-dehydroxylation reactions are shown in Table 1. The range of $T_{OH,b}$ values is lowest for goethites aged at 70°C at pH 6 ($\Delta T_{OH,b}$ = 7.0°C) and pH 11 ($\Delta T_{OH,b}$ = 5.0°C). No relationship exists between $T_{OH,b}$ and coprecipitated Mn or Pb. This suggests that the higher aging temperature may have compensated for the influence that rate of ferrihydrite transformation may have exerted on the stability of goethite during HRTGA analysis.

In contrast, the range in $T_{OH,b}$ was generally greater for samples synthesized at 40°C, especially for samples aged at pH 11 (Table 1). The range of values for $T_{OH,b}$ is 8.0°C for systems aged at pH 6 and $\Delta T_{OH,b}$ = 23.9°C for systems aged at pH 11. The results for experiments at pH 11 and 40°C show a systematic increase in $T_{OH,b}$ with increasing concentration of coprecipitated Mn or Pb. The increase in $T_{OH,b}$ is probably attributable to a decrease in the rate of ferrihydrite transformation with increasing coprecipitated Mn or Pb, which is indicated by the levels of ammonium oxalate extractable Fe remaining in the systems aged at pH 11 and 40°C (Table 1).

The presence of a metal may slow transformation leading to an increased thermal stability by improving goethite crystallinity (Schwertmann, 1984a). As a measure of crystallinity, we also analyzed goethite peak broadening from XRD results. For fine-grained materials, peak broadening may be due to structural defects as well as small particle size (Delhez *et al.*, 1988). We did not attempt to separate the contribution of particle size. We used the width (uncorrected for instrumental broadening) derived from fitting a Lorentzian profile to the goethite (110) Bragg reflection as an indicator of disorder-induced broadening. Plots of peak width *vs.* metal loading for coprecipitated sys-

https://doi.org/10.1346/CCMN.1999.0470309 Published online by Cambridge University Press

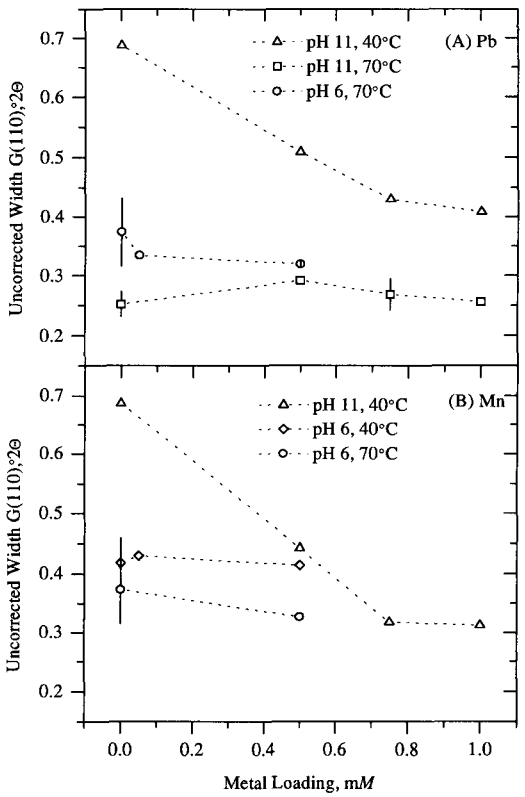

Figure 6. Variation of the uncorrected width of the goethite (110) Bragg reflection. Goethites produced by the transformation of (A) Pb- and (B) Mn-ferrihydrite coprecipitates at various metal loadings, pH, and temperature. Error bars indicate variability between replicate systems.

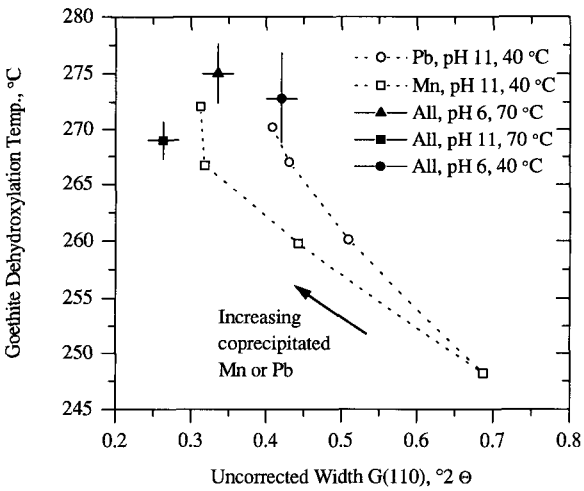

Figure 7. Variation of goethite dehydroxylation temperature as a function of (110) peak broadening. Open symbols are for goethites produced at pH 11, 40°C. Closed symbols are the mean and standard deviation for all samples at the aging conditions indicated.

tems show a dramatic decrease in peak broadening with increasing Pb or Mn at pH 11 and 40°C (Figure 6A and 6B). The influence of the coprecipitated metal at other synthesis conditions was less significant, which is consistent with the smaller variability of $T_{OH,b}$ (Table 1).

A plot of $T_{OH,b}$ as a function of (110) peak broadening for goethites synthesized at pH 11 and 40°C showed a positive relationship between higher coprecipitated metal concentrations and increased thermal stability of goethite (Figure 7). Support for a change in crystallinity *vs.* particle size is provided by comparing $T_{OH,b}$ for goethites synthesized at other aging conditions. Particle dimensions are variable for these goethites, ranging from 5 to 20 nm along the *a* or *b* axes, yet the variability of $T_{OH,b}$ was much lower than for goethites synthesized at pH 11 and 40°C. TEM results confirm that particle size and morphology for an Fe-Mn coprecipitate aged at pH 11, 40°C were similar to the Fe-Pb coprecipitate in Figure 4A (data not shown). Substitution of Mn or Pb into the goethite structure cannot account for the variation in mineral stability. For goethites synthesized at pH 11 and 40°C, total metal substitution determined by chemical dissolution was <2 mole % and varied <1 mole % within a series of metal loadings. Thus, although particle size (or surface area) and metal substitution can influence $T_{OH,b}$ of goethite, crystallization rate apparently plays a predominant role for the goethites formed at pH 11 and 40°C.

CONCLUSIONS

These results indicate that HRTGA is capable of providing information on both bulk structural stability and the distribution of surface structural groups in synthetic goethite. In part, interpretation of goethite thermoanalytical data was limited in previous studies by a lack of instrumental resolution of multiple decomposition reactions. Our thermal analysis results may be interpreted in two possible ways. First, the multiple weight-loss events may be attributed to bulk dehydroxylation events of populations of goethites that vary in crystallite size or crystallinity. Alternatively, a single bulk dehydroxylation may exist that is preceded by a series of weight-loss events due to dehydration-dehydroxylation of surface structural groups.

We believe the latter hypothesis is more reasonable. Whereas the distribution of $=S_1OH$, $=S_2OH$, and $=S_3OH$ will depend on the crystallite morphology, the temperature at which these surface groups decompose should be relatively invariant. The binding energy of these surface groups will not vary regardless of goethite crystallinity. In contrast, $T_{OH,b}$ depends on the long-range atomic order of the crystallite. Thus, $T_{OH,b}$ is sensitive to the type and number of defects that populate the bulk structure as well as crystallite size. The cumulative contributions of these three variables de-

https://doi.org/10.1346/CCMN.1999.0470309 Published online by Cambridge University Press

termine the bulk thermal stability of the goethite crystallite.

The number of surface dehydration-dehydroxylation events in our analytical model is somewhat arbitrary. The actual number of surface dehydration-dehydroxylation events is controlled by the Fe-(oxo)hydroxo bonding environments present on faces that develop during particle growth. Presumably these surface structures are thermally less stable than the bulk structure, since surfaces have unsaturated broken bonds in comparison to the bulk. The fitted temperatures show significant variability for the three surface dehydration-dehydroxylation events for our samples, in part due to differences in the amount of weight loss of the various samples. The response of HRTGA, and thus the temperature of maximum weight loss, depends strongly on the magnitude of the weight loss.

We cannot conclude that the description of the thermal behavior of goethite proposed here is based on the only valid thermal model. However, it is consistent with the available data observed for goethites characterized here and elsewhere. We emphasize that previous research has shown similar *reversible* weight-loss events prior to goethite bulk dehydroxylation (Patterson and Swaffield, 1980). We suggest at least three possible characteristic thermogram profiles for synthetic goethites. For poorly crystalline goethite, bulk dehydroxylation overlaps surface decomposition reactions resulting in an apparent 'single' dehydroxylation event at low temperatures. High-surface area goethite with improved crystallinity shows a 'double' (or multiple) dehydroxylation profile due to a shift of bulk dehydroxylation to higher temperature and significant weight loss from surface-decomposition reactions. Finally, goethites nearly free of structural imperfections possess a 'single' dehydroxylation profile at a high temperature dominated by the bulk decomposition reaction. These profile shapes may be modified by the presence of anionic surface impurities which interfere with true surface dehydration-dehydroxylation reactions (Paterson and Swaffield, 1980; Gasser *et al.*, 1996).

This model for goethite decomposition allows differentiation of surface and bulk (*i.e.*, crystallinity) characteristics of synthetic goethites. The distribution of nonstoichiometric surface water is related to particle morphology. The ability to resolve these weight-loss events suggests that, with proper instrument calibration, binding energies may be determined for various surface species, which may be useful in constraining molecular models for predicting surface-binding constants for oxide minerals (Rustad *et al.*, 1996).

The rate of ferrihydrite transformation appears to exert the primary control on the thermal stability (or crystallinity) of goethite. This was clearly demonstrated for goethites synthesized in the presence of Mn and Pb at pH 11 and 40°C. This observation is supported by examination of Al-substituted goethites, where Al substitution indirectly determined goethite crystallinity (or resistance to dissolution) via retardation of transformation rate (Schwertmann, 1984a). Thus, rapid rates of transformation may account for poor crystallinity in synthetic or natural goethites (Cornell and Giovanoli, 1986).

ACKNOWLEDGMENTS

This work was supported in part by a Graduate Student Research Grant presented to RGF by the Clay Minerals Society, and by Financial Assistance Award Number DE-FC09-96SR18546 from the U.S. Department of Energy to the University of Georgia Research Foundation. We thank L. Keller of MVA, Inc. (Norcross, Georgia) for TEM analyses. This manuscript benefited from constructive, anonymous reviews.

REFERENCES

Anonymous (1997) Appendix B: High resolution TGA option. In *TGA 2950 Thermogravimetric Analyzer Operator's Manual*, TA Instruments, New Castle, Delaware, B1–B76.

Bruemmer, G.W., Gerth, J., and Tiller, K.G. (1988) Reaction kinetics of the adsorption and desorption of nickel, zinc and cadmium by goethite. I. Adsorption and diffusion of metals. *Journal of Soil Science*, **39,** 37–52.

Cambier, P. (1986a) Infrared study of goethites of varying crystallinity and particle size: II. Crystallographic and morphological changes in series of synthetic goehites. *Clay Minerals*, **21,** 201–210.

Cambier, P. (1986b) Infrared study of goethites of varying crystallinity and particle size: I. Interpretation of OH and lattice vibration frequencies. *Clay Minerals*, **21,** 191–200.

Colombo, C., Barron, V., and Torrent, J. (1994) Phosphate adsorption and desorption in relation to morphology and crystal properties of synthetic hematites. *Geochimica et Cosmochimica Acta*, **58,** 1261–1269.

Cornell, R.M. and Giovanoli, R. (1985) Effect of solution conditions on the proportion and morphology of goethite formed from ferrihydrite. *Clays and Clay Minerals*, **33,** 424–432.

Cornell, R.M. and Giovanoli, R. (1986) Factors that govern the formation of multi-domainic goethites. *Clays and Clay Minerals*, **34,** 557–564.

Cornell, R.M., Giovanoli, R., and Schneider, W. (1989) Review of the hydrolysis of iron (III) and the crystallization of amorphous iron(III) hydroxide hydrate. *Journal of Chemical Technology and Biotechnology*, **46,** 115–134.

Cornell, R.M., Posner, R.M., and Quirk, J.P. (1974) Crystal morphology and the dissolution of goethite. *Journal of Inorganic and Nuclear Chemistry*, **36,** 1937–1946.

Cornell, R.M. and Schneider, W. (1989) Formation of goethite from ferrihydrite at physiological pH under the influence of cysteine. *Polyhedron*, **8,** 149–155.

Delhez, R., de Keijser, T.H., Mittemeijer, E.J., and Langford, J.I. (1988) Size and strain parameters from peak profiles: Sense and nonsense. *Australian Journal of Physics*, **41,** 213–227.

Domingo, C., Rodriguez-Clemente, R., and Blesa, M. (1994) Morphological properties of α-FeOOH, γ-FeOOH, and Fe_3O_4 obtained by oxidation of aqueous Fe(II) solutions. *Journal of Colloid and Interface Science*, **165,** 244–252.

Fey, M.V. and Dixon, J.B. (1981) Synthesis and properties of poorly crystalline hydrated aluminous goethites. *Clays and Clay Minerals*, **29,** 91–100.

Forsyth, J.B., Hedley, I.G., and Johnson, C.E. (1968) The magnetic structure and hyperfine field of goethite (α-FeOOH). *Journal of Physics C*, **1,** 179–188.

https://doi.org/10.1346/CCMN.1999.0470309 Published online by Cambridge University Press

Gasser, U.G., Jeanroy, E., Mustin, C., Barres, O., Nuesch, R., Berthelin, J., and Herbillon, A.J. (1996) Properties of synthetic goethites with Co for Fe substitution. *Clay Minerals*, **31,** 465–477.

Giovanoli, R. and Cornell, R.M. (1992) Crystallization of metal substituted ferrihydrites. *Zeitschrift fur Pflanzenernahrung und Bodenkunde*, **155,** 455–460.

Goss, C.J. (1987) The kinetics and reaction mechanism of the goethite to hematite transformation. *Mineralogical Magazine*, **51,** 437–451.

Hiemstra, T., de Wit, J., and van Riemsdijek, W. (1989) Multisite proton adsorption modeling at the solid/solution interface of (hydr)oxides: A new approach II. Application to various important (hydr)oxides. *Journal of Colloid and Interface Science*, **133,** 104–117.

Kuhnel, R.A., Roorda, H.J., and Steensma, J.J. (1975) The crystallinity of minerals—A new variable in pedogenetic processes: A study of goethite and associated silicates in laterites. *Clays and Clay Minerals*, **23,** 349–354.

Mackenzie, R.C., Paterson, E., and Swaffield, R. (1981) Observation of surface characteristics by DSC and DTA. *Journal of Thermal Analysis*, **22,** 269–274.

Manceau, A. and Gates, W.P. (1997) Surface structural model for ferrihydrite. *Clays and Clay Minerals*, **45,** 448–460.

Mann, S., Cornell, R.M., and Schwertmann, U. (1985) The influence of aluminium on iron oxides: XII. High-resolution transmission electron microscopic (HRTEM) study of aluminous goethites. *Clay Minerals*, **20,** 255–262.

Maurice, P.A., Hochella, M.F., Jr., Parks, G.A., Sposito, G., and Schwertmann, U. (1995) Evolution of hematite surface microtopography upon dissolution by simple organic acids. *Clays and Clay Minerals*, **43,** 29–38.

Parfitt, R.L., Russell, J.D., and Farmer, V.C. (1975) Confirmation of the surface structures of goethite (α-FeOOH) and phosphated goethite by infrared spectroscopy. *Journal of the Chemical Society Faraday Transactions I*, **72,** 1082–1087.

Paterson, E. and Swaffield, R. (1980) Influence of adsorbed anions on the dehydroxylation of synthetic goethite. *Journal of Thermal Analysis*, **18,** 161–167.

Reynolds, R.C. (1989) Diffraction by small and disordered crystals. In *Modern Powder Diffraction*, D.L. Bish and J.E. Post, eds., Mineralogical Society of America, Washington, D.C., 145–181.

Rochester, C.H. and Topham, S.A. (1978) Infrared study of surface hydroxyl groups on goethite. *Journal of the Chemical Society Faraday Transactions I*, **75,** 591–602.

Russell, J.D., Parfitt, R.L., Fraser, A.R., and Farmer, V.C. (1974) Surface structures of gibbsite, goethite, and phosphated goethite. *Nature*, **248,** 220–221.

Rustad, J.R., Felmy, A.R., and Hay, B.P. (1996) Molecular statics calculation of proton binding to goethite surfaces: A new approach to estimation of stability constants for multisite surface complexation models. *Geochimica et Cosmochimica Acta*, **60,** 1563–1576.

Sampson, C.F. (1969) The lattice parameters of natural single crystal and synthetically produced goethite (α-FeOOH). *Acta Crystallographica*, **B25,** 1683–1685.

Schulze, D.G. (1984) The influence of aluminum on iron oxides. VIII. Unit-cell dimensions of Al-substituted goethites and estimation of Al from them. *Clays and Clay Minerals*, **32,** 36–44.

Schulze, D.G. and Schwertmann, U. (1984) The influence of aluminum on iron oxides: X. Properties of Al-substituted goethites. *Clay Minerals*, **19,** 521–539.

Schulze, D.G. and Schwertmann, U. (1987) The influence of aluminum on iron oxides: XIII. Properties of goethites synthesized in 0.3 M KOH at 25°C. *Clay Minerals*, **22,** 83–92.

Schwertmann, U. and Murad, E. (1983) Effect of pH on the formation of goethite and hematite from ferrihydrite. *Clays and Clay Minerals*, **31,** 277–284.

Schwertmann, U. (1984a) The influence of aluminum on iron oxides: IX. Dissolution of Al-goethites in 6 M HCl. *Clay Minerals*, **19,** 9–19.

Schwertmann, U. (1984b) The double dehydroxylation peak of goethite. *Thermochimica Acta*, **78,** 39–46.

Schwertmann, U., Cambier, P., and Murad, E. (1985) Properties of goethites of varying crystallinity. *Clays and Clay Minerals*, **33,** 369–378.

Schwertmann, U. and Taylor, R.M. (1989) Iron oxides. In *Minerals in Soil Environments*, J.B. Dixon and S.B. Weeds, eds., Soil Science Society of America, Madison, Wisconsin, 379–438.

Schwertmann, U. (1990) Some properties of soil and synthetic iron oxides. In *Soil Colloids and Their Associations in Aggregates*, M.F. de Boot, M.H.B. Hayes, and A. Herbillon, eds., Plenum Press, New York, 57–103.

Schwertmann, U. and Cornell, R.M. (1991) *Iron Oxides in the Laboratory: Preparation and Characterization*, VCH, Weinheim, 137 pp.

Sposito, G. (1984) *The Surface Chemistry of Soils*, Oxford University Press, New York, 234 pp.

Wolska, E. and Schwertmann, U. (1993) The mechanism of solid solution formation between goethite and diaspore. *Neues Jahrbuch fur Mineralogie-Monatshefte*, **5,** 213–223.

(Received 15 January 1998; accepted 18 November 1998; Ms. 98-008)

https://doi.org/10.1346/CCMN.1999.0470309 Published online by Cambridge University Press